the ability of Si to undergo π bonding to oxygen.[15]

Experimental Section

Preparation of 1,2-Mo_2(O-*i*-Pr)$_2$(OAr)$_4$ (I). To a solution of Mo_2(O-*i*-Pr)$_6$ (1.48 g, 2.8 mmol) in benzene (50 mL) was added 2,6-dimethylphenol (HOAr, 2.55 g, 20.9 mmol), and the mixture was allowed to stir for 4 h. Removal of solvent under vacuum, followed by addition of hexane (20 mL), filtration, and cooling to −15 °C gave large red crystals of product.

^{1}H NMR (30 °C, C_6D_6)[2] δ 6.6–7.0 (m, $OC_6H_3Me_2$), 2.28 (s, $OC_6H_3Me_2$), 5.10 (septet, $OCHMe_2$), 1.11 (d, $OCHMe_2$). A great deal of difficulty was experienced in trying to obtain clean ^{1}H NMR spectra of this compound. The solution spectra changed slowly over time, showing the buildup of a number of new species. Two of these components were identified from their spectra as 2,6-dimethylphenol and $Mo_2(OAr)_6$ (II) with trace amounts of 2-propanol.

Preparation of $Mo_2(OAr)_6$ (II). By use of the same procedure as above, the solution was stripped and a melt formed between I and the excess phenol at 100 °C for 10 min. Addition of hexane gave the product as an insoluble red powder. Anal. Calcd for $Mo_2C_{48}O_6H_{54}$: C, 62.75; H, 5.92. Found: C, 62.20; H, 6.01. ^{1}H NMR (30 °C, C_6D_6) δ 6.6–7.1 (m, $OC_6H_3Me_2$), 2.09 (s, $OC_6H_3Me_2$).

X-ray Structural Determination for 1,2-Mo_2(O-*i*-Pr)$_2$(OAr)$_4$ (I). General procedures have been described previously.[16]

A dark red crystal of dimensions 0.25 × 0.30 × 0.30 mm was selected and transferred to the cold stream of the goniostat under an atmosphere of dry nitrogen. The cell dimensions obtained from 36 reflections at −163 °C with Mo Kα (λ = 0.71069 Å) were a = 18.169 (6) Å, b = 11.327 (3) Å, c = 10.678 (3) Å, α = 99.58 (2)°, β = 57.82 (2)°, γ = 97.63 (2)°, Z = 2, d(calcd) = 1.441 g cm^{-3} with space group $P\bar{1}$.

A total number of 4810 reflections were collected by using standard moving-crystal moving-detector techniques with the following values: scan speed = 4.0° min^{-1}; scan width = 2.0 + dispersion; single background time at extremes of scan = 4 s; aperture size = 3.0 × 4.0 mm. The limits of data collection were $6° < 2\theta < 45°$. Of the 4810 reflections, 4731 were unique, and the number with $F > 2.33\sigma(F)$ was 3758.

The structure was solved by direct methods and refined by full-matrix techniques, including all hydrogen atoms, to give final residuals $R(F)$ = 0.0425 and $R_w(F)$ = 0.0406. The goodness of the fit for the last cycle was 1.223, and the maximum Δ/σ was 0.05.

Acknowledgment. We thank the donors of the Petroleum Research Fund, administered by the American Chemical Society, and the Research Corp. for support of this work.

Registry No. I, 86645-80-9; II, 86667-99-4; Mo_2(O-*i*-Pr)$_6$, 62521-20-4; Mo, 7439-98-7.

Supplementary Material Available: Tables of anisotropic thermal parameters and lists of observed and calculated structure factors (38 pages). Ordering information is given on any current masthead page.

(15) Chisholm, M. H.; Reichert, W. W.; Thornton, P. *J. Am. Chem. Soc.* **1978**, *100*, 2744.
(16) Huffman, J. C.; Lewis, L. N.; Caulton, K. G. *Inorg. Chem.* **1980**, *19*, 2755.

Contribution from the Centre de Recherches Nucléaires, 67037 Strasbourg Cedex, France

^{161}Dy Mössbauer Spectroscopy Studies of Divalent and Trivalent Dysprosium Halides and Oxyhalides

J. M. FRIEDT,* J. MacCORDICK, and J. P. SANCHEZ

Received February 8, 1983

^{161}Dy hyperfine interaction measurements are reported for the dysprosium dihalides DyX_2, trihalides DyX_3, and oxyhalides DyOX (X = Cl, Br, I) using the 26-keV Mössbauer resonance. In the dihalides, the electron configuration of dysprosium is divalent ($4f^{10}$). However, it has been impossible to obtain pure phases of these compounds. The oxyhalides order antiferromagnetically below 10 K. The hyperfine parameters and the magnetic ordering in these compounds are interpreted in terms of electronic structure with use of a Hamiltonian including electric crystal field and magnetic exchange effects. The change of mean square nuclear radius of ^{161}Dy between the ground and 26-keV levels ($\Delta\langle r^2\rangle = 8.0 \times 10^{-3}$ fm^2) is deduced by combination of the isomer shift results with free-ion electron density calculations.

Introduction

Considerable interest has been devoted recently to the problem of the existence of lanthanide (Ln) ions in valence states other than the common trivalent configuration $4f^n$.[1-5] Whereas the existence and the stability of the divalent Ln^{2+} configuration are well established for the elements of the middle (Sm, Eu) and of the end (Yb) of the lanthanide series, the behavior of some of the other elements is still debated. In halides of composition $LnX_{2\pm x}$, a saltlike character and the occurrence of a valence configuration $4f^{n+1}$ has been demonstrated for the elements Nd, Sm, Eu, Tm, and Yb. On the other hand, for some other elements (e.g. La, Gd), substoichiometric halides $LnX_{2\pm x}$ present a metallic character; this has been concluded from measurements of conductivity, optical absorption, etc.[6] In the latter class of materials, the Ln ion appears to be trivalent, with delocalized electrons responsible for the metallic character.[6] Other substoichiometric halides of the type $LnX_{1\pm x}$ (e.g. LaCl or Er_4I_5) present peculiar structures consisting of metallic clusters with interstitial halide atoms. The Ln ions are probably also trivalent in these systems.[7]

Dysprosium represents a limiting case in this range of behavior since thermodynamic calculations predict that the divalent configuration Dy^{2+} might be at the limit of stability in halide compounds.[8] The existence of a dysprosium chloride, $DyCl_2$, phase and of intermediate chlorides has been established from phase diagram studies.[9] Although conductivity

(1) Haschke, J. M. In "Handbook on the Physics and Chemistry of Rare Earths"; Gschneider, K. A., Jr., Eyring, L., Eds.; North-Holland: Amsterdam, 1979; Vol. IV, p 89.
(2) Johnson, D. A. *Adv. Inorg. Chem. Radiochem.* **1977**, *20*, 1.
(3) Bärnighausen, H.; Warkentin, E. *Rev. Chim. Miner.* **1973**, *10*, 141.
(4) Bärnighausen, H. *Proc. Rare Earth Res. Conf., 12th* **1976**, *1*, 404.
(5) Bärnighausen, H. private communication of unpublished results. Bossert, W. Ph.D. Thesis, University of Karlsruhe, 1981. Gütlich, P.; Link, R.; Ensling, J., private communication of unpublished results.
(6) Corbett, J. D. *Rev. Chim. Miner.* **1973**, *10*, 239.
(7) Simon, A. *Angew. Chem., Int. Ed. Engl.* **1980**, *20*, 1.
(8) Kim, Y. C.; Oishi, J. *J. Less-Common Met.* **1979**, *65*, 199.

0020-1669/83/1322-2910$01.50/0

measurements of DyI_2 were not clearly conclusive,[10] the existence of the Dy^{2+} valence configuration in DyI_2, $DyBr_2$, and $DyCl_2$ (actually Dy_5Cl_{11}) is strongly supported by structural investigation, i.e. from the comparison of the bond lengths with the sums of the ionic radii.[4,5]

Mössbauer spectroscopy represents a versatile and sensitive method for characterizing the valence configuration of atoms in solids. For instance, the presence of different valence states of the Ln atoms has been clearly demonstrated in several mixed-valence compounds of europium (e.g. Eu_3S_4, Eu_3O_4, or Eu_4Cl_9). The electron configuration of Dy is trivalent in all insulating solids measured until now; isomer shifts of the ^{161}Dy (26-keV) Mössbauer resonance in the range from −0.4 to 0.8 mm/s relative to DyF_3 have been reported in compounds.[11] A preliminary estimate for the isomer shift of the Dy^{2+} and Dy^{4+} valence configurations is available from impurity studies in CaF_2 and GdF_3 hosts, respectively.[12,13]

In the present work, we have applied the 26-keV Mössbauer resonance of ^{161}Dy to the investigation of the nature of the dysprosium valence configurations in the divalent halides DyX_2 (X = Cl, Br, I). The physical existence of the divalent dysprosium configuration in these solids is unambiguously demonstrated from the measured isomer shift. Combining this measurement with free-ion electron density calculations reported in the literature, we deduce a value of 8.0×10^{-3} fm^2 for the change in mean square nuclear radius of the ^{161}Dy nucleus between the ground and 26-keV levels.

It is found that the synthesis of the divalent dysprosium halides is very delicate; it turned out to be impossible to obtain pure phases. This finding also agrees with reports by other authors. In order to allow a proper characterization of the impurity phases that always contaminate our DyX_2 samples, we have completed our study by an investigation of the ^{161}Dy Mössbauer spectra in the trihalides DyX_3 and in the oxyhalides DyOX (X = Cl, Br, I). The latter class of compounds has been found to present an antiferromagnetic ordering below 10 K. The hyperfine parameters and magnetic properties and their relationship to electronic structure are discussed for these latter compounds.

Experimental Section

General Procedures. Handling and transfer operations involving moisture- and air-sensitive compounds were carried out in a glovebox under dried argon. Dysprosium metal for synthesis (99.99%, Johnson-Matthey) was employed as freshly prepared filings from an ingot under argon. Iodine and bromine for halogen–metal reactions were of analytical reagent grade; bromine was vacuum distilled prior to use (see below).

Preparation of Compounds. (a) Dihalides. $DyCl_2$ was prepared by reduction of the anhydrous trichloride with the metal.[9] A stoichiometric mixture of the reactants in a tantalum boat was sealed under 1 atm of Ar in a quartz tube and heated for 40 h at 700–720 °C. Care was taken to avoid prolonged heating above the apparent peritectic temperature of 721 °C in order to reduce possible subsequent phase transformations in $DyCl_2$ and generation of nonstoichiometric species.[4,9]

$DyBr_2$ was synthesized by interaction of the elements in stoichiometric proportions in a quartz tube sealed under vacuum ($\sim 5 \times 10^{-5}$ torr). This was accomplished by distillation of bromine from an ampule onto previously heated (~200 °C) and degassed Dy filings contained in a separate compartment of a Stock-type vacuum manifold. The reaction mixture was first heated in the course of 8 h to 500 °C in a t °C/20 °C temperature gradient, permitting gradual reaction of bromine vapor with the metal. Uptake of bromine was rapid above 225 °C and complete at the upper temperature limit. In a second step, the tube was heated uniformly to 575 °C during 2–3 h and axially rotated in order to homogenize the viscous melt formed at ~550 °C. The melt was then quenched to room temperature.

DyI_2 has been obtained both by reduction of the triiodide with dysprosium metal[6] and by oxidation of Dy with HgI_2.[3] Preliminary experiments using these methods showed that the reaction products were not crystallographically pure and that the reactions had not gone to completion, thus confirming previous observations. Purer samples of the diiodide were produced by stoichiometric interaction of the elements sealed under vacuum or under dry argon in a quartz tube. In this case, the reaction mixture was heated in two steps in the manner described above for the dibromide, whereby a final melt temperature of 660 °C was required. However, the necessity of this higher temperature in the attainment of suitable reaction and homogenization conditions apparently favored partial reaction with silica, resulting in the formation of DyOI. Although trivalent impurities could never be entirely eliminated, the best diiodide preparations were finally obtained by prolonged reaction of intimate Dy–DyI_3 mixtures in sealed tantalum tubes.[5]

(b) Trihalides. The anhydrous compounds DyX_3 (X = Cl, Br, I) were obtained by thermal dehydration of the corresponding halide hydrates in the presence of ammonium halides under vacuum.[14,15] DyI_3 was also prepared directly from the elements by following the method of Asprey et al.[16]

(c) Oxyhalides. DyOCl and DyOBr were readily prepared in satisfactory purity by published procedures.[17,18] However, attempts to make pure DyOI by starting from Dy_2O_3 or by using a method analogous to that for the corresponding europium compound[19] were not successful. The oxyiodide could only be obtained in pure form as a residue of the sublimation of partially hydrolyzed DyI_3.[5]

X-ray Diffraction Data. Powdered samples of all products were mounted in 0.3- or 0.5-mm quartz capillaries and examined by the Debye–Scherrer technique using Cu Kα radiation and a camera of diameter 114.6 mm. Powder patterns were indexed and lattice parameters calculated and checked against those of known structural data (Table I). The "$DyCl_2$" sample actually appears to be predominantly the intermediate Dy_5Cl_{11} phase of the $DyCl_2$–$DyCl_3$ system.[4] Of the dihalides, $DyBr_2$ was generally obtained as the purest material; trivalent components (DyOI, DyI_3) were always present in the diiodide.[3]

ac Magnetic Susceptibility Measurements. The ac susceptibility data were obtained in the temperature range 4.2–40 K, with a conventional mutual-inductance bridge operating at 197.6 Hz.[22] The determination of the absolute susceptibility using a calibration substance was not performed (thus precluding the determination of the effective paramagnetic moment of Dy in our samples). However, the magnetic data provide information on the type of magnetic ordering

Table I. Crystallographic Data of DyX_2, DyX_3, and DyOX (X = Cl, Br, I)

compd	struct type	detected impurities	ref
Dy_5Cl_{11}	vernier	DyOCl?	4
$DyBr_2$	SrI_2		1, 4
DyI_2	$CdCl_2$	DyOI, DyI_3	3
$DyCl_3$	$AlCl_3$	...	20
$DyBr_3$	BiI_3	...	21
DyI_3	BiI_3	...	16
DyOCl	PbFCl	...	17
DyOBr	PbFCl	...	18
DyOI	PbFCl	...	3

(9) Corbett, J. D.; Mc Collum, B. C. *Inorg. Chem.* **1966**, *5*, 938.
(10) Johnson, D. A.; Corbett, J. D. *Colloq. Int. C.N.R.S.* **1970**, *No. 180*, 429.
(11) Bauminger, E. R.; Kalvius, G. M.; Nowik, I. In "Mössbauer Isomer Shifts"; Shenoy, G. K., Wagner, F. E. Eds.; North Holland: Amsterdam, 1978; Chapter 10, p 663.
(12) Henning, W.; Kaindl, G.; Kienle, P.; Koerner, H. J.; Kulzer, H.; Rehm, K. E.; Edelstein, N. *Phys. Lett. A* **1968**, *28A*, 209.
(13) Cohen, R. L.; Guggenheim, H. J. *Nucl. Instrum. Methods* **1969**, *71*, 27.
(14) Kutscher, J.; Schneider, A. *Inorg. Nucl. Chem. Lett.* **1971**, *7*, 851.
(15) Taylor, M. D. *Chem. Rev.* **1962**, *62*, 503.
(16) Asprey, L. B.; Keenan, T. K.; Kruse, F. H. *Inorg. Chem.* **1964**, *3*, 1137.
(17) Templeton, D. H.; Dauben, C. H. *J. Chem. Soc.* **1953**, *75*, 6069.
(18) Mayer, I.; Zolotov, S.; Kassierer, F. *Inorg. Chem.* **1965**, *4*, 1637.
(19) Bärnighausen, H. *J. Prakt. Chem.* **1961**, *14*, 313.
(20) Templeton, D. H.; Carter, G. F. *J. Phys. Chem.* **1954**, *58*, 940.
(21) Brown, D. In "Halides of Lanthanides and Actinides"; Wiley: New York, 1968.
(22) The collaboration of J. L. Tholence (CRTBT, Grenoble, France) in performing the ac susceptibility measurements is gratefully acknowledged.

Table II. ^{161}Dy Mössbauer Parameters of "Dy_5Cl_{11}"[a]

	δ_{IS}, mm/s	H_{hf}, kOe	e^2qQ, mm/s	W, mm/s	% a
		4.2 K			
Dy^{2+}	−5.8 (2)		50–60[c]	7[b]	70 (10)
Dy^{3+}	0.8 (2)	5560 (30)	123 (10)	6.5 (5)	30 (10)
		300 K			
Dy^{2+}	−5.8 (2)			6 (1)	45 (10)
Dy^{3+}	0.8 (2)			8 (1)	55 (10)

[a] δ_{IS} is the isomer shift given with respect to DyF_3, H_{hf} is the hyperfine field, e^2qQ is the quadrupole coupling constant fitted by assuming H_{hf} parallel to q, W is the fwhm of the resonance line(s), and a is the relative resonance area of the Dy ions in a given configuration. Errors in the last figures are given in parentheses. [b] Fixed value. [c] The Dy^{2+} ions in Dy_5Cl_{11} are both seven- and eight-coordinated.

at T_c and permit calculation of the paramagnetic Curie temperatures by assuming a simple Curie–Weiss behavior above T_c.

^{161}Dy Mössbauer Measurements. The measurements were performed on samples (mounted in tight aluminum capsules with indium seals) with use of the 26-keV resonance of Dy on natural dysprosium absorbers of 50–100 mg of Dy/cm^2. The source, consisting of neutron-irradiated (6 days in a flux of 2×10^{13} n cm^2 s^{-1}) $^{160}Gd^{162}DyF_6$ (50 mg), was kept at 300 K and moved sinusoidally in synchronization with an 800-channel analyzer triggered in the time mode. Continuous variation of the absorber temperature was possible in the range 1.5–300 K. The Mössbauer spectra were recorded for several maximum-velocity spans (e.g., ranges of ±50, ±170, and ±250 mm/s) and computer analyzed to sums of suitable Lorentzian line shapes. Relative intensities and energies of the absorption lines were constrained to the theoretical value for the type of hyperfine interaction considered. The nuclear parameters (quadrupole and magnetic moments) were selected according to the review by Stevens and Dunlap.[23]

Results and Discussion

(a) Mixed-Valent Dy_5Cl_{11} and Dihalides of Dysprosium ($DyBr_2$, DyI_2). Dy_5Cl_{11}. Results of Mössbauer spectra of this compound recorded at selected temperatures in the range 4.2–300 K are shown in Figure 1 and Table II. The 4.2 K Mössbauer spectrum can be interpreted as a superposition of two quadrupole-split spectral components of equal isomer shifts $\delta_{IS} = -5.8$ mm/s (about 70% of the total resonance area) and of a magnetic type subspectrum with $\delta_{IS} = 0.8$ mm/s. The unusual isomer shift of −5.8 mm/s (with respect to DyF_3) for the quadrupole subspectra is attributed to the divalent configuration of dysprosium ions;[11,12,24] the magnetic contribution arises from slowly relaxing Dy^{3+} ions.

At higher temperature ($T \geq 77$ K), a progressively increasing contribution of Dy^{3+} confers overall asymmetry to a broad resonance line (Figure 1b,c). Owing to the relaxation behavior of the Dy^{3+} ions, the spectral shape at 77 K is complex and analysis of the data becomes unreliable. The room-temperature spectrum can be satisfactorily represented as a sum of two single Lorentzian lines, the trivalent contribution being predominant and the divalent component appearing as a shoulder of about 42% relative intensity (Figure 1c).

According to extensive X-ray diffraction studies performed by Baernighausen,[4] Dy_5Cl_{11} can be classified as a mixed-valence compound, with Dy^{2+}:Dy^{3+} = 4:1; it belongs to a general class of "vernier"-type structures where Dy^{2+} and Dy^{3+} ions appear in both seven- and eight-coordinate sites.[1] The observation of two subspectra for the Dy^{2+} component (Table II) is consistent with the crystal structure of Dy_5Cl_{11}, which presents several crystallographically nonequivalent lattice sites.[4] The somewhat high Dy^{3+} contribution (30% instead of 20% of the expected total resonance area) deduced from the 4.2 K Mössbauer data,[25] together with the significant decrease

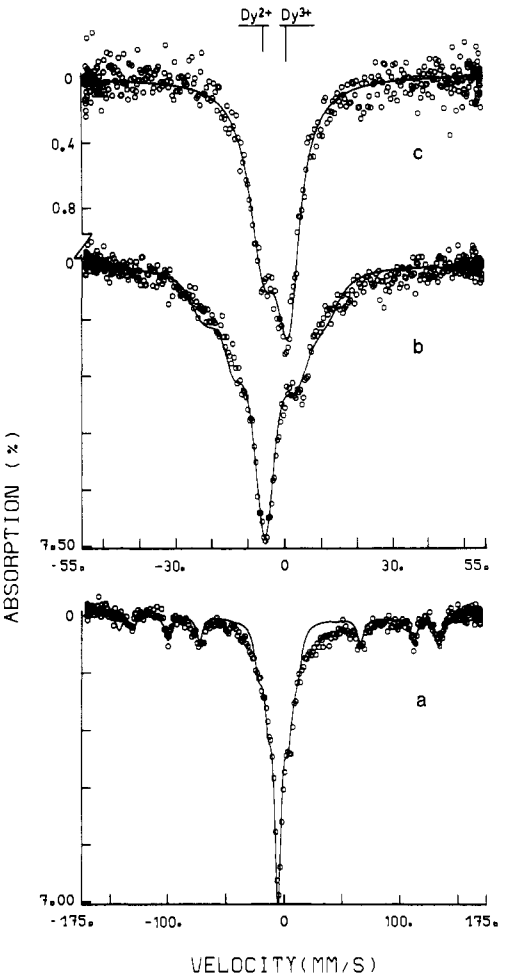

Figure 1. ^{161}Dy Mössbauer spectra of "Dy_5Cl_{11}" at different temperatures and velocity ranges: (a) 4.2 K and ±175 mm/s; (b) 4.2 K and ±55 mm/s; (c) 300 K and ±55 mm/s.

of the relative area of the Dy^{2+} component with increasing temperature (Table II), indicates that our Dy_5Cl_{11} sample contains a spurious trivalent dysprosium impurity with a relatively high Debye temperature.

An estimate for the Debye temperatures (θ_D) of the two valence states in Dy_5Cl_{11} is available by reference to an europium mixed-valence, vernier-type compound: in Eu_4Cl_9,[5] ^{151}Eu Mössbauer spectroscopy (which is technically much better suited for θ_D measurements than ^{161}Dy spectroscopy) provided values of 150 and 170 K for the θ_D's of the Eu^{2+} and Eu^{3+}, sites, respectively. Direct application of these θ_D's for the two types of ions in Dy_5Cl_{11} is insufficient to account for the observed temperature dependence of the Dy^{2+}:Dy^{3+} spectral area ratio. However, the results as a whole can only be understood in terms of the impurity phase DyOCl (10% in our best sample), for which θ_D is estimated to be $\simeq$300 K from the temperature dependence of the ^{161}Dy spectral area in the pure oxyhalide. In our purest Dy_5Cl_{11} sample, the presence of DyOCl could not be ascertained from X-ray powder diffraction owing to the coincidence of the most intense reflections of DyOCl with those of Dy_5Cl_{11}. On the other hand, powder patterns readily revealed the presence of DyOCl in less pure samples.

$DyBr_2$. The Mössbauer measurements for $DyBr_2$ in the low-velocity range ±55 mm/s are represented in Figure 2b–d.

(23) Stevens, J. G.; Dunlap, B. D. *J. Phys. Chem. Ref. Data* **1976**, *5*, 1093.
(24) Friedt, J. M.; MacCordick, J.; Sanchez, J. P.; Rebizant, J. *Solid State Commun.* **1980**, *35*, 1021.

(25) The spectral area (a) is proportional to the Debye–Waller factor (f) and the number of resonant atoms (n) in a given configuration: $a_i \approx nf_i$. At 4.2 K it is safe to assume that the f_i's saturate to a nearly common value, therefore $a_i(4.2\ K) \approx n_i$.

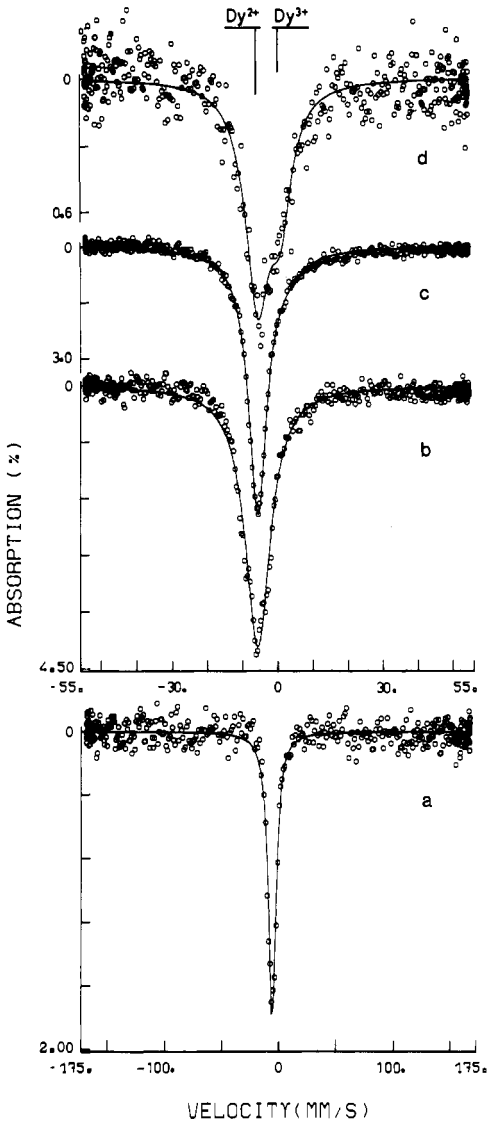

Figure 2. ^{161}Dy Mössbauer spectra of $DyBr_2$ at different temperatures and velocity ranges: (a) 4.2 K and ±175 mm/s; (b–d) 4.2, 77, and 300 K, respectively, and ±55 mm/s.

At 4.2 K, the Mössbauer spectrum reveals a single resonance line with an isomer shift of −5.6 mm/s, which is characteristic for Dy^{2+} ions. Higher velocity span measurements (±170 mm/s) at 4.2 K (Figure 2a) reveal no other component within experimental accuracy (a proportion of 10–15% Dy^{3+}, which would behave magnetically at this temperature, can escape detection). As in the case of Dy_5Cl_{11}, the progressive degree of asymmetry observed with increasing temperature in the right flank of the absorption is indicative of the gradual appearance of a Dy^{3+} component. In contrast with the case for Dy_5Cl_{11}, the Dy^{2+} spectral area remains predominant at 300 K (Table III, Figure 2d). The 77 and 300 K spectra were fitted as a sum of two resonance lines. The presence of Dy^{3+}, which is evidenced at 77 and 300 K, is attributed to a low-level (≤10%) DyOBr impurity. This contribution (magnetic subspectrum) would be indistinguishable from the base line at 4.2 K because of the low intensity of all the spectral lines. The temperature dependence of the Dy^{2+} and Dy^{3+} spectral areas is accounted for by respective Debye temperatures of ~150 and ~300 K and a temperature-independent ratio of the two valence states: $n(Dy^{2+})/n(Dy^{3+}) = 0.9$.

DyI_2. The 4.2 K ^{161}Dy Mössbauer spectra of the best DyI_2 sample show a very weak magnetic component in addition to a broad central contribution (Figure 3a). As mentioned above, the X-ray results reveal the presence of DyI_3 and DyOI phases

Table III. ^{161}Dy Mössbauer Parameters of "$DyBr_2$" at Different Temperatures[a]

	δ_{IS}, mm/s	W, mm/s	% a
	4.2 K		
Dy^{2+}	−5.6 (2)	8.5 (5)	100 (10)
	77 K		
Dy^{2+}	−5.6 (2)	6.5 (10)	85 (10)
Dy^{3+}	0.9 (2)	14 (1)	15 (10)
	300 K		
Dy^{2+}	−5.6 (2)	8 (1)	63 (10)
Dy^{3+}	0.9 (2)	8 (1)	37 (10)

[a] The symbols have the same meaning as in Table II.

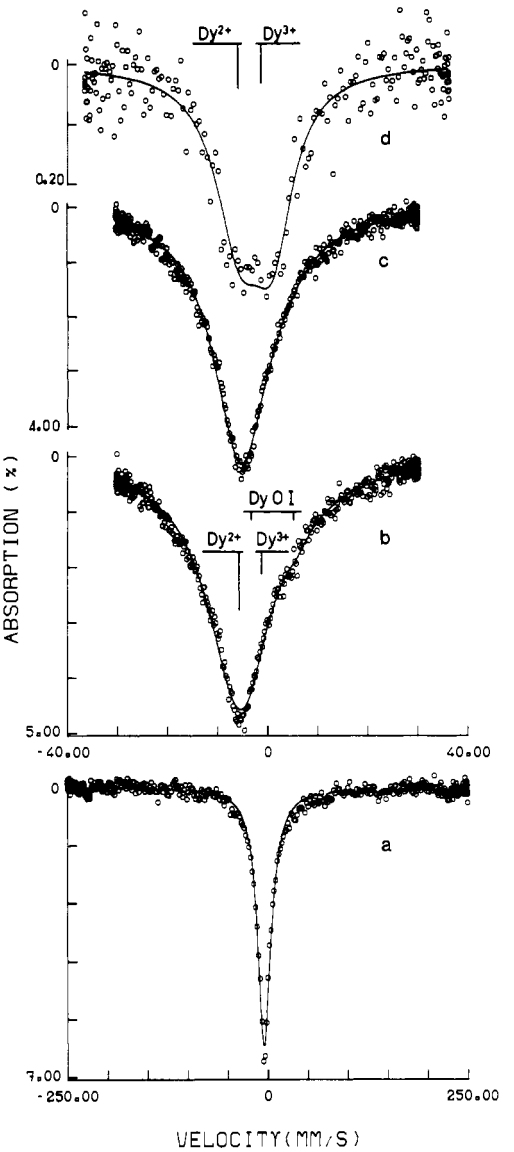

Figure 3. ^{161}Dy Mössbauer spectra of DyI_2 at different temperatures and velocity ranges: (a) 4.2 K and ±250 mm/s; (b–d) 4.2, 77, and 300 K, respectively, and ±40 mm/s.

in all the samples prepared (Table I). The experimental 4.2 K data can be straighforwardly represented by assuming a superposition of the contribution from DyI_3 and DyOI impurities and a single line with the unusual isomer shift of −5.6 mm/s characteristic of Dy^{2+} ions (Table IV). This type of data analysis has been performed consistently for measurements over different velocity ranges (Figure 3a,b), with hyperfine interaction parameters of the DyI_3 and DyOI impurities constrained in the fitting procedure to the values determined independently for these phases (see below).

Table IV. ^{161}Dy Mössbauer Parameters of the "DyI_2" Sample at Different Temperatures[a]

	δ_{IS}, mm/s	H_{hf}, kOe	e^2qQ, mm/s	W, mm/s	% a
		4.2 K			
Dy^{2+}	−5.6 (3)			18 (2)	72 (10)
Dy^{3+} (DyOI)	1.25[b]	5713[b]	108[b]	5[b]	6 (3)
Dy^{3+} (DyI_3)	1[b]			30[b]	22 (10)
		77 K			
Dy^{2+}	−5.6 (3)			12 (2)	80 (10)
Dy^{3+}	1[b]			18 (2)	20 (10)[c]
		300 K			
Dy^{2+}	−5.6 (5)			12 (2)	55 (10)
Dy^{3+}	1[b]			10 (2)	45 (10)

[a] The symbols have the same meaning as in Table II. [b] Parameters constrained in the analysis. [c] Value underestimated owing to difficulty of representing broadening effects due to paramagnetic relaxation by a Lorentzian line shape.

At higher temperatures (77 and 300 K), the Mössbauer spectra consist basically of two superimposed single lines, one with the isomer shift corresponding to Dy^{2+} and the other with $\delta_{IS} \simeq 1$ mm/s (Figure 3c,d). The latter line corresponds to DyI_3 and DyOI, which are shown independently to give rise in this temperature range to broad and coinciding single resonances. Here again, the strong decrease of the Dy^{2+} spectral area with increasing temperature is due to the relatively low Debye temperature of the Dy^{2+} component (~150 K) compared to that of DyOI (~300 K).

It is of interest to mention that an independent study of dysprosium dihalides by ^{161}Dy Mössbauer spectroscopy by Gütlich, Link, and Ensling in 1977 provided experimental results very comparable to the present ones.[5]

Discussion. In the previous section, the spectral component of the Mössbauer spectra of Dy_5Cl_{11}, $DyBr_2$, and DyI_2 with an isomer shift in the range −5.8 to −5.6 ± 0.2 mm/s was attributed to the contribution by Dy^{2+} ions. The near-constancy of the isomer shifts (δ_{IS}) throughout the series of dihalides indicates that covalent admixture in these compounds must be small. It is concluded that the isomer shift $\delta_{IS} \simeq -5.7$ ± 0.4 mm/s with respect to DyF_3 is representative for the Dy^{2+} free-ion isomer shift value. The isomer shift between the Dy^{2+} ($4f^{10}$) and Dy^{3+} ($4f^9$) ionic states is proportional to the product of the difference of relativistic electronic densities[26] for the two configurations and the isomer shift calibration constant α:[11]

$$\delta_{IS}[Dy^{2+}\text{–}Dy^{3+}] = \alpha\, \Delta\rho(0)[Dy^{2+}\text{–}Dy^{3+}] \qquad (1)$$

Using the appropriate value of $\Delta\rho(0) = -45.73a_0^3$ [26] and the isomer shifts of −5.7 mm/s and 0 (with respect to DyF_3) for the ionic Dy^{2+} and Dy^{3+} configurations, one obtains $\alpha = 0.125a_0^3$ mm/s; from these data, one deduces a value for the change of the mean square nuclear charge radius between the excited and ground states: $\Delta\langle r^2\rangle = +8.0 \times 10^{-3}$ fm^2.

This $\Delta\langle r^2\rangle$ value is consistent with an estimate of $\Delta\langle r^2\rangle = +7.9 \times 10^{-3}$ fm^2, which was based on $\delta_{IS} = 7.0 \pm 0.4$ mm/s for Dy^{4+} ions in GdF_3[13] and from the computation of $\Delta\rho(0)[Dy^{4+}\text{–}Dy^{3+}] = 56.67a_0^3$.[26] The small difference between our $\Delta\langle r^2\rangle$ value and that quoted in the literature[11] ($\Delta\langle r^2\rangle = +7.4 \times 10^{-3}$ fm^2) corresponds to the use of different $\Delta\rho(0)$ computations and represents essentially the uncertainty of the calibration procedure for the δ_{IS} expression (eq 1).

The quadrupole splittings reported for the Dy^{2+} component in Dy_5Cl_{11} and the single-line broadening observed in DyI_2 (single-line fit of 18 mm/s at 4.2 K, which is to be compared to an experimental minimum width of 4 mm/s) is attributed to electric field gradient (EFG) effects acting at the nucleus of cations with this valence state. Calculation of the electronic contribution to the EFG provides a quadrupole coupling constant of $e^2Qq^{4f}(1 - R) = 60$ mm/s for the $Dy^{2+}(^5I_8)$ free ion ($|J_z = 8\rangle$).[27] This value is not inconsistent with the above measurements, since in a solid e^2qQ may be reduced with respect to the free-ion value by the crystal field and often by the lattice contribution to the EFG. These two factors are also reflected in the smaller line width observed in $DyBr_2$ (8.5 mm/s at 4.2 K), because of a smaller EFG in $DyBr_2$ than in DyI_2. The temperature dependences of the quadrupole coupling constant or of the line widths of the Dy^{2+} ion in all three compounds, Dy_5Cl_{11}, $DyBr_2$, and DyI_2, is qualitatively explained by reduction of the EFG with increasing temperature, via thermal population of crystal field levels. It is not clear whether paramagnetic relaxation effects, which certainly account for the temperature dependence of the Dy^{3+} line width, can be invoked in the case of the Dy^{2+} ion since the latter is a non-Kramers ion.

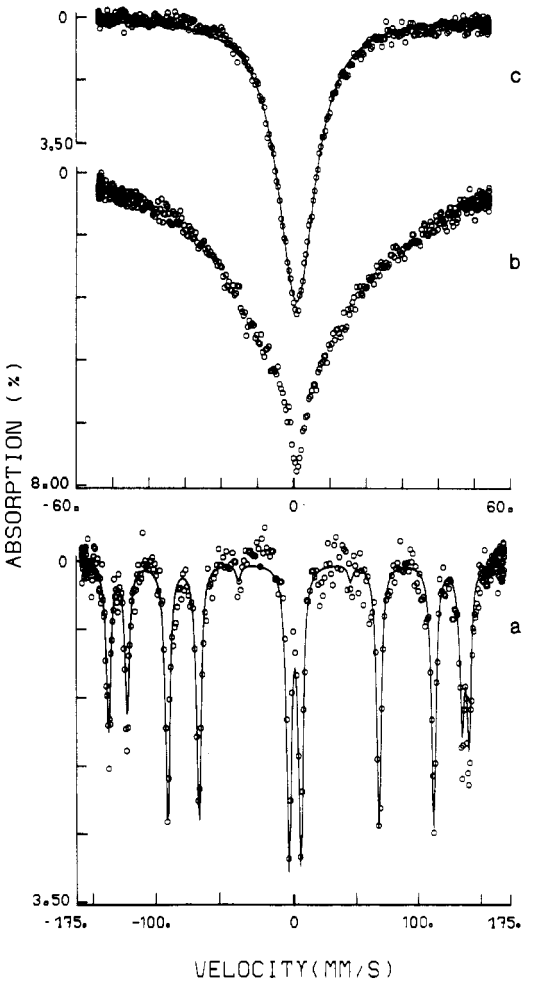

Figure 4. ^{161}Dy Mössbauer spectra of DyOCl at various temperatures and velocity ranges: (a) 4.2 K and ±175 mm/s; (b, c) 77 and 300 K, respectively, and ±60 mm/s.

(b) Oxyhalides of Dy(III): DyOCl, DyOBr, and DyOI. The ^{161}Dy Mössbauer spectra of DyOCl at various temperatures are shown in Figure 4. The oxyhalides DyOBr and DyOI behave similarly. The 4.2 K Mössbauer data reveal well-resolved magnetic spectra and are described by combined magnetic and quadrupole interactions (Table V, , Figure 4a). This behavior is not unexpected since Dy^{3+} is a Kramers ion,

(26) Band, I. M.; Fomichev, V. I. *At. Data Nucl. Data Tables* **1979**, *23*, 296.

(27) Bleaney, B. In "Magnetic Properties of Rare-Earth Metals"; R. J. Elliott, R. J., Ed.; Plenum Press: London, 1972; Chapter 8, p 383.

Table V. ^{161}Dy Mössbauer Parameters of DyOX (X = Cl, Br, I) at 4.2 K and Magnetic Data Deduced from ac Susceptibility Measurements

	δ_{IS}, mm/s	H_{hf}, kOe	e^2qQ, mm/s	W, mm/s	T_N, K	θ, K
DyOCl	0.94 (10)	5682 (10)	115 (2)	4.4 (2)	9.5 (5)	−21 (1)
DyOBr	0.98 (10)	5682 (10)	110 (2)	4.3 (2)	7.5 (5)	−7 (1)
DyOI	1.25 (10)	5713 (10)	108 (2)	4.3 (2)	9.5 (5)	−24 (1)

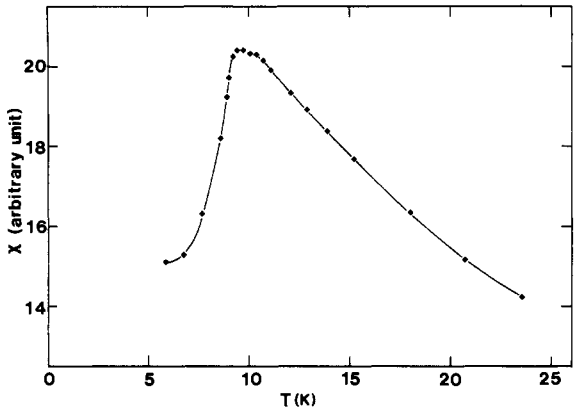

Figure 5. ac susceptibility of DyOCl as a function of temperature.

for which all crystalline electric field states are at least doublets. Therefore, the observation of magnetically split spectra does not necessarily imply that these compounds order magnetically at low temperature; indeed, magnetic hyperfine structure is usually observed at such low temperatures in paramagnetic compounds of dysprosium because the electronic spin relaxation is slow in comparison to the nuclear Larmor precession.

This ambiguity of interpretation is resolved from low-temperature ac susceptibility measurements. It is concluded from peaks in ac susceptibility that the three oxyhalides are antiferromagnets; their respective transition temperatures T_N are summarized in Table V. Above T_N the susceptibilities obey a Curie-Weiss law with a negative paramagnetic Curie temperature (θ), indicating predominant antiferromagnetic interactions (Figure 5 Table V). The occurrence of magnetic order in DyOCl below T_N = 9 K has been observed previously.[28]

In Mössbauer spectroscopy, the hyperfine spectra below and immediately above the ordering temperatures are identical, indicating the occurrence of paramagnetic relaxation behavior at $T \gtrsim T_N$. At 77 K, the transition rates between the Dy crystal field levels are not fast enough to cancel completely the effect of the magnetic interactions The spectral shape at 77 K is interpreted as a pure quadrupole interaction (~50 mm/s) with lines broadened by the still fluctuating magnetic field.[29,30] However, a detailed relaxation analysis of the data obtained at this single temperature would be meaningless because of the planar character of the **g** tensor (see below $g_\parallel << g_\perp$), which requires considerably more exacting treatment than the common uniaxial situation.[31] At 300 K, broad (W = 12.5 (5) mm/s for DyOCl) single resonance lines are observed (Figure 4c). These broadenings arise from the lattice and 4f electric gradients and possibly also from residual relaxation effects. Inspection of Table V shows that the hyperfine interaction parameters of all three dysprosium oxyhalides are nearly identical. The small spread of isomer shifts indicates that covalency effects are minute within this class of compounds, as is common in rare-earth derivatives.

It is interesting to consider a theoretical analysis of the hyperfine parameters and of the magnetic properties of this series of compounds (Table V) using an electronic Hamiltonian that includes the effects of the electrical crystal field (CEF) and of the magnetic exchange:

$$\mathcal{H}_{el} = \mathcal{H}_{CEF} + \mathcal{H}_{exch} \quad (2)$$

Indeed, an estimate for the CEF parameters has become recently available from optical spectroscopy of rare-earth impurity elements in several isostructural oxyhalides.[32]

In the C_{4v} symmetry of the dysprosium site in the PbFCl structure type, the CEF Hamiltonian is written in the notation of Racah operators as

$$\mathcal{H}_{CEF} = B_0^2C_0^2 + B_0^4C_0^4 + B_4^4(C_4^4 + C_{-4}^4) + B_0^6C_0^6 + B_4^6(C_4^6 + C_{-4}^6) \quad (3)$$

$$C_q^k = \left(\frac{4\pi}{2k+1}\right)^{1/2} Y_q^k$$

We have selected the CEF parameters reported for Tb^{3+} impurities in GdOCl, i.e. $B_0^2 = -943$ cm^{-1}, $B_0^4 = -634$ cm^{-1}, $|B_4^4| = 694$ cm^{-1}, $B_0^6 = 787$ cm^{-1}, and $|B_4^6| = 264$ cm^{-1},[32] since the structural parameters are closely similar to those of our systems. It is noteworthy that the CEF parameters determined for other rare-earth elements or oxyhalides hosts do not depend significantly on the nature of the specific system. Therefore, the above set of parameters is considered to provide representative results for all three dysprosium oxyhalides in the present context.

The magnetic-exchange Hamiltonian in eq 2 is assumed to be isotropic and is written in the molecular field approximation as

$$\mathcal{H}_{exch} = -g_J\mu_B \vec{J}\cdot\vec{H}_{mol} \quad (4)$$

The value and the orientation of H_{mol} were treated as variable parameters in the data analysis. Equation 2 provides a set of electronic eigenfunctions and their energies which permit calculation of the hyperfine parameters and their temperature dependence.[33,34]

The magnetic hyperfine field at the ^{161}Dy nucleus is described as a sum of the three following contributions:

$$H_{hf} = H_{4f} + H_{cp} + H_N \quad (5)$$

where H_{4f} represents the sum of the orbital and spin-dipolar contributions produced by the open 4f shell. Core polarization (H_{cp}) is much smaller than H_{4f} and is proportional to the latter ($\vec{S} = (g_J - 1)\vec{J}$). H_N includes all the contributions from neighboring ions (supertransferred field) and is considered negligible. Thus, H_{hf} is proportional to the thermal average of the orbital angular momentum ($\langle J_z \rangle$). It is calculated from the electronic wave functions (Γ_i) and energies (E_i) with use of eq 2 as

(28) Elmaleh, D.; Fruchart, D.; Joubert, J. C. *J. Phys. (Orsay, Fr.)* **1971**, *32*, C1, 741.
(29) Almog, A.; Bauminger, E. R.; Levy, A.; Nowik, I.; Ofer, S. *Solid State Commun.* **1973**, *12*, 693.
(30) Stewart, G. A.; Wortmann, G. *Phys. Lett. A* **1981**, *85A*, 185.
(31) Wickman, H. H.; Wertheim, G. K. In "Chemical Applications of Mössbauer Spectroscopy"; Goldanskii, V. I. Herber, R. H. Eds.; Academic Press: New York, 1968; p 576.
(32) Holsä, J.; Porcher, P. *J. Chem. Phys.* **1981**, *75*, 2108; **1982**, *76*, 2790, 2798. These authors have used the Wybourne notation. The relationship between the notations of tensor operators (Racah) and of the operator equivalent method (Stevens) is given by: Kassman, A. J. *J. Chem. Phys.* **1970**, *53*, 4118.
(33) Ofer, S.; Nowik, I.; Cohen, S. G. In "Chemical Applications of Mössbauer Spectroscopy"; Goldanskii, V. I.; Herber, R. H., Eds.; Academic Press: New York, 1968; p 428.
(34) Friedt, J. M.; Shenoy, G. K.; Dunlap, B. D. *J. Phys. (Orsay, Fr.)* **1979**, *40*, C2, 243.

$$H_{hf} = \frac{\sum_i \langle \Gamma_i|J_z|\Gamma_i\rangle e^{-E_i/kT}}{J\sum_i e^{-E_i/kT}} H_{FI} \quad (6)$$

where the free-ion hyperfine field (H_{FI} corresponding to $J_z = {}^{15}/_2$) has been estimated as 6320 kOe from electronic radial distribution calculations, which includes relativistic contributions.[34,35]

The electric field gradient at the Dy nucleus is a sum of an electronic and a lattice contribution:

$$q_z = (1 - R)q^{4f} + (1 - \gamma_\infty)q^{lat}\frac{3\cos^2\theta - 1}{2} \quad (7)$$

θ is the angle between q^{lat} and the 4f magnetic moment direction. R and γ_∞ are respectively the Sternheimer shielding and antishielding coefficients.

The lattice contribution can be estimated empirically from the quadrupole interaction measured in the isostructural GdOX compound since Gd^{3+} is an S-state ion where $q^{4f} = 0$. Scaling for the nuclear quadrupole moments, we calculate the lattice contributions $(1 - \gamma_\infty)e^2q^{lat}(Q(^{161}Dy))$ to be +21.7 ± 2, +32.6 ± 0.5, and +33.5 ± 0.5 mm/s in DyOCl, DyOBr, and DyOI, respectively.[34,36]

The electronic contribution (q^{4f}) can be calculated for each of the electronic wave functions Γ_i by application of the electric field gradient operator as[33,34]

$$q^{4f}{}_i = -\langle J||\alpha||J\rangle\langle\Gamma_i|3\hat{J}_z{}^2 - \hat{J}^2|\Gamma_i\rangle\langle r^{-3}\rangle_{4f} \quad (8)$$

Since electronic relaxation within the Γ_i levels is fast in comparison to the Larmor precession time, the temperature dependence of q^{4f} is described by a thermal average over the populated levels as

$$q^{4f}(T) = \frac{\sum_i q^{4f}{}_i e^{-E_i/kT}}{\sum_i e^{-E_i/kT}} \quad (9)$$

The CEF part alone of the Hamiltonian (eq 2) provides a well-isolated Kramers doublet represented by the values

$$|\Gamma_g\pm\rangle = -0.388|\pm{}^7/_2\rangle + 0.888|\pm{}^1/_2\rangle - 0.245|\pm{}^9/_2\rangle$$

The first excited doublet is at 172 K, with a wave function

$$|\Gamma_1\pm\rangle = -0.006|\mp{}^{13}/_2\rangle - 0.102|\mp{}^{11}/_2\rangle + 0.260|\mp{}^5/_2\rangle + 0.717|\mp{}^3/_2\rangle - 0.350|\pm{}^3/_2\rangle - 0.532|\pm{}^5/_2\rangle + 0.050|\pm{}^{11}/_2\rangle + 0.012|\pm{}^{13}/_2\rangle$$

The other levels are calculated to be at much higher energy. The calculated strong admixture of angular momentum states arises obviously from the comparable magnitudes of the diagonal and nondiagonal terms corresponding to the reported CEF parameters ($B_0{}^4$, $B_0{}^6$ vs. $B_4{}^4$, $B_4{}^6$, respectively). It should be noted that Γ_g gives rise to a small moment along the CEF principal axis ($g_\parallel{}^g = 0.36$) whereas the in-plane g component is large ($g_\perp{}^g = 10.16$). This calculation is consistent with the perpendicular moment orientation with respect to the crystal c axis reported from preliminary neutron-scattering work.[28]

Strong wave function mixing is induced by exchange field splitting of these two doublets. This result in an anisotropic **g** tensor that is sensitively affected by the modulus and the orientation of $\vec{H}_{mol}$. Systematic calculations of $H_{hf}(T)$ and $q^{4f}(T)$ have been performed within the ^6H ground level with use of the Hamiltonian (eq 2) for changing value and orientation of $\vec{H}_{mol}$. A maximum of moment (i.e. of H_{hf}) is found for polar angles $\theta = 90°$, $\varphi = 45°$ for the orientation of $\vec{H}_{mol}$ with respect to the system of CEF (i.e. crystallographic) axis. This orientation corresponds most likely to the magnetic structure since it provides a minimal energy in the limits of the approximations of the above calculations. It is also consistent with the neutron-diffraction results for DyOCl.[28] It may further be noted that the dysprosium moment deduced from neutron scattering (8.6 ± 0.2 μ_B) is in agreement with the present evaluation from H_{hf}, i.e. 8.9 μ_B.

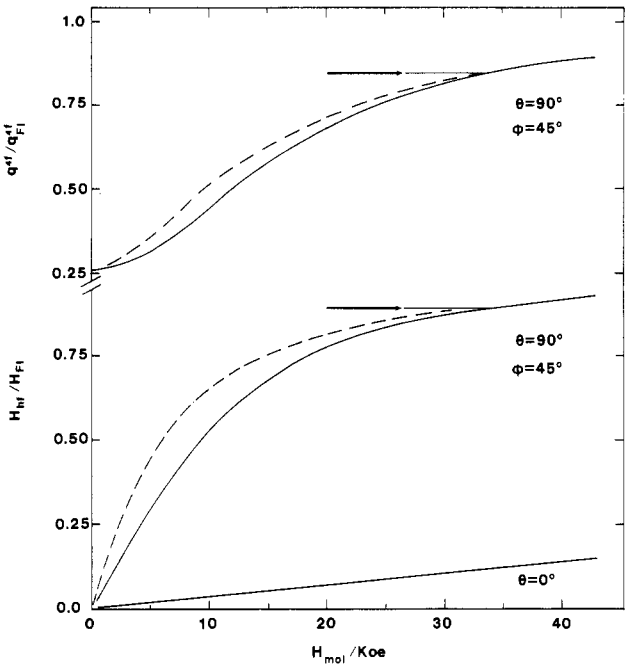

Figure 6. Reduced hyperfine field and 4f electric field gradient calculated at two temperatures (2 and 4 K) as a function of the intensity of the molecular field (H_{mol}). The orientation of $\vec{H}_{mol}$ vs. CEF axis is $\theta = 90°$, $\varphi = 45°$. The experimental values are indicated by arrows. For comparison, the reduced H_{hf} dependence is also represented with $\vec{H}_{mol}$ along the crystal c axis.

Assuming perpendicular orientation between magnetic moment and the CEF principal axis, one obtains the following experimental values for dysprosium oxychloride (θ in eq 7 is 90°) (Table V):

$$H_{hf}(4.2\text{ K})/H_{FI} = 0.89$$

$$e^2(1 - R)(q^{4f}(4.2\text{ K}))Q = 126\text{ mm/s} = 2610\text{ MHz}$$

The same values are observed within limits of error in the other two oxyhalides. With a free-ion ($|J_z = {}^{15}/_2\rangle$) quadrupole coupling constant $e^2(1 - R)q^{4f}{}_{FI}Q = 150$ mm/s,[34] the reduced value of the 4f contribution to the field gradient is $q^{4f}(4.2\text{ K})/q^{4f}{}_{FI} = 0.84$.

Figure 6 represents the calculated reduced hyperfine field and 4f electric gradient as a function of the magnitude of the molecular field at 2 and 4 K ($\vec{H}_{mol}$ being at polar angles $\theta = 90°$, $\varphi = 45°$ vs. CEF axis). For completeness, the calculated reduced H_{hf} is also represented for the hypothetical situation of $\vec{H}_{mol}$ along the crystal c axis. Excellent agreement between measured and calculated hyperfine parameters is found when a value of 33 kOe is selected for H_{mol}.

The above fitted value for H_{mol} is in surprisingly good agreement with the prediction from simple molecular field theory. Indeed, the latter provides an estimate of $H_{mol} = [3kT_N\langle J_x\rangle/g_J\mu_B J(J + 1)] = 32$ kOe for a Néel temperature $T_N = 9.5$ K and a saturation moment of 8.6 μ_B.

(35) Dunlap, B. D. In "Mössbauer Effect Methodology"; Gruverman, I. J., Ed.; Plenum Press: New York, 1971; Vol. 7, p 123.
(36) Katila, T. E.; Typpi, V. K.; Shenoy, G. K.; Niinisto, L. *Solid State Commun.* **1972**, *11*, 1147. The gadolinium oxyhalides were remeasured in: Czjzek, G., private communication. He finds the same value for q^{lat} as in the above reference but with opposite sign.

Table VI. ^{161}Dy Mössbauer Parameters of DyX_3 (X = Cl, Br, I) at Different Temperatures[a]

	$DyCl_3$		$DyBr_3$		DyI_3	
	δ_{IS}, mm/s	W, mm/s	δ_{IS}, mm/s	W, mm/s	δ_{IS}, mm/s	W, mm/s
4.2 K	0.8 (2)	23.0 (5)	1.0 (2)	23.3 (5)	0.7 (2)	29.0 (5)
77 K	0.8 (2)	12 (1)	0.9 (2)	12 (1)	1.0 (2)	15 (1)
300 K	0.7 (2)	7.5 (10)	not measd		0.9 (2)	9.5 (10)

[a] $DyCl_3$ and $DyBr_3$ were prepared by dehydration of the corresponding hydrated halides; DyI_3 was obtained by direct synthesis from the elements.

Finally, it may be pointed out that the B_0^2 parameter in the CEF Hamiltonian is directly related to the lattice field gradient q^{lat}.[32-34]

$$B_0^2 = -\frac{q^{lat}\langle r^2\rangle(1-\sigma_2)}{2(1-\gamma_\infty)} \qquad (10)$$

With the same shielding coefficients ($(1-\gamma_\infty)/(1-\sigma_2) = 112$) and radial integral ($\langle r^2\rangle = 0.206 \times 10^{-16}$ cm^2) used previously for $Dy(OH)_3$,[34] one estimates B_0^2 in the range from -584 to -893 cm^{-1} for DyOCl and DyOI, respectively. This is to be compared to the value of -943 cm^{-1} deduced from the optical work[32] as used above. Such slight disagreement is not really surprising, owing to the empirical nature of the known shielding coefficients σ_2 and γ_∞. It is of greater importance that the sign of B_0^2 deduced from the two independent methods is consistent. In view of the very different CEF levels probed by optical and Mössbauer spectroscopy, the overall agreement in the above description of the hyperfine parameters is satisfactory.

In summary, it is found that the hyperfine parameters, the optical data and the magnetic properties of the series of dysprosium oxyhalides can be evaluated with reasonable consistency by the crystal field method. Further knowledge of the electronic properties of these materials could be obtained from investigations of the crystal field effects with use of information provided by inelastic neutron scattering or specific heat. It should be noted that the analysis of the combined optical, hyperfine, and magnetic results is coherent for the two different systems ($Dy(OH)_3$[34] and the present oxyhalides) when a common set of atomic parameters such as are necessary for the interpretation of the experimental results is used (H_{FI}, q^{4f}_{FI}, σ_2, γ_∞; eq 6, 9, 10). A test of the general applicability of these parameters would be of considerable interest, particularly with respect to other insulating materials. However, the presently available data from the literature are insufficient for this purpose.

(c) Halides of Dy(III): $DyCl_3$, $DyBr_3$, and DyI_3. The Mössbauer spectra of $DyCl_3$ and $DyBr_3$ (obtained by dehydration) and of DyI_3 (direct synthesis from the elements) show similar temperature dependences (Figure 7). All three compounds reveal a broad single resonance line at 4.2 K (Table VI). With increasing temperature, the resonance line width gradually decreases; however, at 300 K, it remains broader than the minimum experimental line width (~4 mm/s). The major source of line broadenings observed at low temperatures arises from electronic paramagnetic relaxation effects, while the residual broadening at 300 K may be attributed to the lattice (and possibly 4f) EFG which is temperature independent (respectively -31.3 ± 0.5 mm/s and -36.9 ± 0.5 mm/s for $DyBr_3$ and DyI_3 as estimated from ^{155}Gd data on the isostructural GdX_3 comounds[36]).

Samples of DyI_3 prepared by the dehydration method behave differently. They present at 4.2 K a well-developed relaxation pattern (Figure 8a). The values of the average hyperfine field and quadrupole coupling constant (5660 ± 10 kOe and 100 ± 2 mm/s respectively) suggest a ground-state

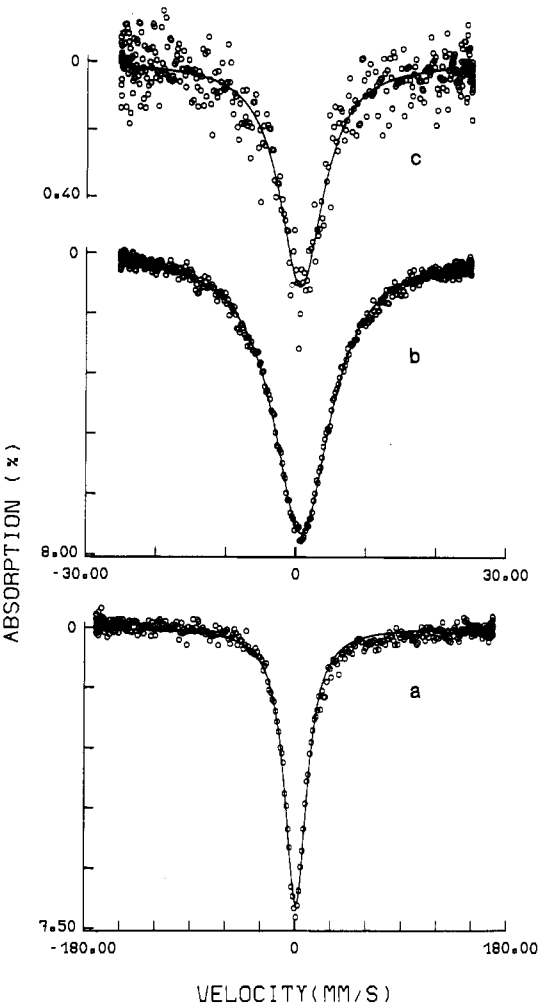

Figure 7. ^{161}Dy Mössbauer spectra of $DyCl_3$ at different temperatures and velocity ranges: (a) 4.2 K and ±180 mm/s; (b, c) 77 and 300 K, respectively, and ±30 mm/s.

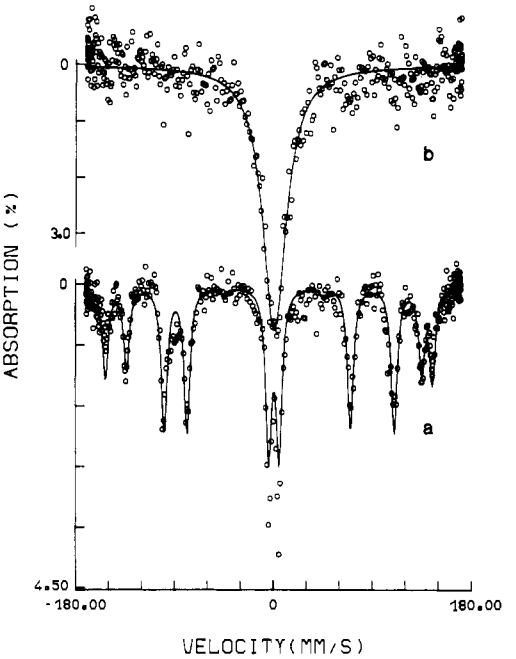

Figure 8. ^{161}Dy Mössbauer spectra at different DyI_3 samples at 4.2 K: (a) sample prepared by dehydration of the hydrated iodide; (b) sample prepared by direct synthesis from the elements.

level with a predominant character $|J_z = \pm^{15}/_2\rangle$. The influence of the preparation procedure of the sample on the electronic

relaxation rate of Dy^{3+} ions in DyI_3 is not understood at present. In any event, both types of samples showed identical and correct X-ray powder diffraction patterns. The absence of detectable amounts of moisture or coordinated H_2O was established from infrared spectra. Furthermore, low-temperature ac susceptibility measurements showed that the various DyI_3 samples were paramagnetic down to 4.2 K ($\theta = -5 \pm 1$ K).

The lack of slow paramagnetic relaxation in the three compounds $DyCl_3$, $DyBr_3$, and DyI_3 at a temperature as low as 4.2 K is unusual for insulating compounds.[33] This can be tentatively explained in terms of the high point symmetry occurring at the Dy site in these crystals, which should give rise to a **g** tensor that is not largely anisotropic.[37] Hence, the relaxation rate is faster than in most compounds that present a large **g** anisotropy.[33,37]

The different relaxation behaviors observed in the two nominally identical samples of DyI_3 can conceivably be assigned to undetectable lattice defects. These may occur in a larger proportion in the dehydrated samples; the consequent lowering of local symmetry could then be responsible for an anisotropic **g** tensor and hence longer relaxation times. Alternatively, undetected paramagnetic impurities might contaminate the DyI_3 samples prepared by direct synthesis from the elements and thus be responsible for faster relaxation rate in this sample.[38]

Summary and Conclusions

The existence of the Dy^{2+} ($4f^{10}$) valence configuration of dysprosium in the solid dihalides (Dy_5Cl_{11}, $DyBr_2$, and DyI_2) is unambiguously demonstrated from the isomer shift measured ^{161}Dy Mössbauer spectroscopy. The occurrence of unresolved quadrupole interactions and the absence of paramagnetic relaxation effects confirm this assignment. Unfortunately, none of these phases could be obtained entirely pure. The mixed-valence state of Dy in Dy_5Cl_{11} and the unavoidable presence of impurities whose Debye temperatures differ widely from that of the Dy^{2+} sites complicate the interpretation of the temperature-dependent Mössbauer data. This difference of lattice vibration modes for the different sites is responsible for the unusual increase of the spectral contribution of the Dy^{3+} sites as the temperature is increased from 4.2 to 300 K.

Investigations are also reported for the dysprosium trihalides and oxyhalides. The Mössbauer study of trihalides is restricted to isomer shift measurements because of the occurrence of paramagnetic relaxation effects in the whole range of temperatures from 4.2 to 300 K.

The oxyhalides have been shown to order antiferromagnetically at temperatures below 10 K. The low-temperature (4.2 K) hyperfine parameters (hyperfine field and electric field gradient) are interpreted in terms of a crystal field Hamiltonian consistent with optical and magnetic data. Paramagnetic hyperfine structures persist at temperatures well above T_N, as is common for insulating dysprosium compounds.

Acknowledgment. The collaboration of J. Rebizant, Euratom, Karlsruhe, West Germany, in performing the X-ray diffraction measurements and analysis is gratefully acknowledged. We thank Professor Bärnighausen and W. Kuhn, University of Karlsruhe, for providing samples of DyI_2 and DyOI for comparison with our own preparations. We thank Professors Bärnighausen, Gütlich, Link, and Ensling for communicating unpublished results on $DyCl_2$ and $DyBr_2$ which are comparable to our own.

Registry No. ^{161}Dy, 13967-68-5; Dy_5Cl_{11}, 60616-39-9; $DyBr_2$, 83229-05-4; DyI_2, 36377-94-3; DyOCl, 14986-29-9; DyOBr, 15923-91-8; DyOI, 50652-54-5; $DyCl_3$, 10025-74-8; $DyBr_3$, 14456-48-5; DyI_3, 15474-63-2.

(37) See, e.g.: Altschuler, S. A.; Kozyrev, B. M. In "Electronic Paramagnetic Resonance in Compounds of Transition Elements"; Wiley: New York, 1974; pp 403-4.
(38) Bhargava, S. C.; Knudsen, J. E.; Morup, S. *J. Phys. Chem. Solids* **1979**, *40*, 45.

Contribution from the Department of Chemistry, University of Tennessee, Knoxville, Tennessee 37996-1600

Interactions of the Carbonylbis(triphenylphosphine)rhodium(I) Cation with Purine–Pyrimidine Base Pairs As Studied by Carbon-13, Phosphorus-31, and Proton NMR

DAVID W. ABBOTT and CLIFTON WOODS*

Received December 20, 1982

The interactions of the electrophile $[(PPh_3)_2(CO)Rh]^+$ (denoted as Rh(I)) with purine–pyrimidine base pairs have been investigated with use of ^{13}C, ^1H, and $^{31}P\{^1H\}$ NMR analyses. Nucleoside stability orders for the electrophile have been found to be cytidine (N(3)) > guanosine (O(6)) > adenosine (N(1)) >> thymidine and uridine. Since coordination of Rh(I) to guanosine (Guo) occurs at O(6), the relative order of stability of the Guo and adenosine (Ado) interactions is somewhat surprising. The hydrogen bonding between Guo and cytidine (Cyd) has been shown to be strong enough to prevent the total breakdown of the Guo–Cyd base pair upon addition of Rh(I) to 1:1 nucleoside mixtures. In 1:1:1 Guo–Cyd–Rh(I) mixtures a complex set of equilibria exists involving Guo–Rh(I), Cyd–Rh(I), and Guo–Cyd interactions. As Cyd is added to the 1:1:1 Guo–Cyd–Rh(I) mixture, the Cyd–Rh(I) interaction increases and the Guo–Rh(I) interaction decreases, with the Guo being more extensively involved in hydrogen bonding with the excess Guo. In 1:1:2 mixtures of Guo–Cyd–Rh(I), the Guo–Rh(I) and Cyd–Rh(I) interactions are present in equal amounts. When triethylamine is added to 1:1:1 Guo–Cyd–Rh(I) mixtures, deprotonation of Guo occurs and the equilibria shift away from the Cyd–Rh(I) interaction in favor of the Rh(I)–guanosinate interaction. The effects of Rh(I) on purine–pyrimidine base pairs are discussed in terms of the possible relevance to antitumor behavior of metal complexes through hydrogen bond disruption and base mispairing in DNA.

Introduction

We have recently shown that the electrophile $[(PPh_3)_2(CO)Rh]^+$ will interact with purine nucleoside derivatives in $(CD_3)_2SO$ to form complexes of the type $[Rh(PPh_3)_2(CO)(L)]PF_6$ (L = purine nucleoside).[1] One observation of this previous study that is of particular interest is the binding of the Rh(I) cation to O(6) of guanosine (Guo) in neutral $(CD_3)_2SO$ solution. We have also shown that coordination

(1) Abbott, D. W.; Woods, C. *Inorg. Chem.* **1983**, *22*, 597.

0020-1669/83/1322-2918$01.50/0